Journal of Materials Chemistry C

PAPER

View Article Online
View Journal | View Issue

A highly efficient UV photodetector based on a ZnO microwire p–n homojunction

Cite this: J. Mater. Chem. C, 2014, 2, 5005

Linlin Shi,[ab] Fei Wang,[ab] Binghui Li,*[a] Xing Chen,[a] Bin Yao,[c] Dongxu Zhao*[a] and Dezhen Shen[a]

Received 24th December 2013
Accepted 13th April 2014

DOI: 10.1039/c3tc32547d

www.rsc.org/MaterialsC

A highly efficient ultraviolet photodetector was successfully obtained based on a Sb-doped p-type ZnO microwire p–n homojunction which consisted of a single Sb-doped p-type ZnO microwire and a single undoped ZnO microwire. The ultralong Sb-doped ZnO single crystalline microwires were synthesized *via* a chemical vapor deposition method. The ZnO microwire homojunction showed well-defined rectification characteristics, which indicated the p-type conductivity of the Sb-doped ZnO microwire. An ultraviolet photodetector with an external quantum efficiency of 64.5% was obtained based on the ZnO microwire p–n homojunction. The photodetector showed high wavelength selectivity with a full width at half maximum of 6 nm for the photoresponse peak located at 386 nm.

1. Introduction

As a direct wide band-gap semiconductor, ZnO has drawn great attention due to its potential applications in ultraviolet (UV) optoelectronic devices, including UV light emission diodes,[1,2] laser diodes,[3,4,17] and detectors.[5,6,9–13] Compared with other semiconductors such as GaN and GaAs, ZnO has high internal photoconductive gain and high resistance to high-energy particle irradiation.[7,8] Due to these properties, ZnO is considered a promising material to fabricate high sensitivity UV photodetectors, which could be utilized in chemical and biological analyses, flame detection, optical communications, and astronomical studies.

Because the stable and reproducible p-type doping of ZnO is still a great challenge, the reports based on the ZnO p–n homojunction photodetector have been extremely limited until now. Most ZnO UV photodetectors are of the photoconductive type,[9,10] or based on the metal–semiconductor Schottky junction.[11–13] Photoconductive detectors usually exhibit a low dark current and high photocurrent gain, owing to the absorption and desorption process of surface states. But their response speeds are quite slow, which could seriously hinder the device performance. Schottky junction photodetectors have a relatively high response speed but their high dark current could result in reducing sensitivity. To obtain high performance semiconductor detectors, the p–n junction is an ideal device structure, since p–n junction photodetectors usually have advantages of high sensitivity, fast responding speed,[33] low dark current, and high stability in the atmosphere.[34] Recently, much effort has been made to obtain high quality p-type ZnO. Some research groups have demonstrated that large-mismatched Sb atoms are efficient p-type dopants for ZnO nanowires,[14–16] and an electrically pumped UV nanolaser based on Sb-doped ZnO nanowires has been obtained.[17]

In this work, we synthesized ultralong Sb-doped p-type ZnO single crystalline microwires with an average length of 10 millimeters. A p–n homojunction UV photodetector was fabricated by crossing a single Sb-doped and a single undoped ZnO microwire together. The fine rectification characteristics were obtained on the p–n homojunction. The UV photodetector exhibited perfect wavelength selectivity with a full width at half maximum (FWHM) of only 6 nm. The peak responsivity of this UV photodetector is 200 mA W^{-1} at 386 nm under −5 V bias, which showed the external quantum efficiency (EQE) of 64.5%.

2. Experimental section

2.1 Synthesis of ZnO microwire

Sb-doped ZnO microwires were grown by a catalyst-free chemical vapor deposition (CVD) method with a two-zone tube furnace. ZnO and graphite powders were thoroughly mixed with a weight ratio of 1 : 1, then the mixture was put into an alumina boat to act as the reactant source material. The Sb_2O_3 powders which served as the dopant source material were loaded into another boat at the upstream to ensure that Sb_2O_3 and ZnO powders could vaporize at the same speed. A 100 nm ZnO film was deposited on the Si substrate by the sputtering method, and

[a]State Key Laboratory of Luminescence and Applications, Changchun Institute of Optics, Fine Mechanics and Physics, Chinese Academy of Sciences, No. 3888 Dongnanhu Road, Changchun, 130033, People's Republic of China. E-mail: zhaodx@ciomp.ac.cn; binghuili@163.com; Fax: +86-431-86176312; Tel: +86-431-86176312

[b]Graduate University of the Chinese Academy of Sciences, Beijing 100049, People's Republic of China

[c]Department of Physics, Jilin University, Changchun 130023, People's Republic of China

then the substrate was loaded above the ZnO powders. During the synthesis progress, the two sources were loaded into the furnace at different temperature zones with a constant flow of 100 sccm argon (99.99%) as the carrier gas. The reactant ZnO source was heated to 1100 °C and the Sb_2O_3 dopant source was heated to 600 °C, simultaneously. When the ZnO source was heated to about 1000 °C, oxygen was introduced with a 30 sccm flow rate for about 2 min to keep the synthesis under the oxygen-rich conditions which would suppress the formation of Sb_O. After maintaining the source temperature for 40 min, the furnace was turned off and cooled down to room temperature. After the growth, ultralong ZnO microwires with an average length of about 10 millimeters were observed on the substrate. The synthesis of the undoped ZnO microwires follows the same procedure without the Sb dopant source.

2.2 Device fabrication

To fabricate a p–n homojunction UV photodetector, a single Sb-doped ZnO microwire and a single undoped ZnO microwire were placed overlapping each other on the glass substrate to form a crossed structure, then fixed with indium electrodes at each end.

2.3 Measurements

The morphology of the ZnO microwires was characterized by a field-emission scanning electron microscope (FE-SEM) (model: Hitachi S-4800) equipped with an X-ray energy dispersive spectrometer (EDX). The selected area electron diffraction (SAED) patterns were obtained on a JEOL JEM-2100F. Photoluminescence (PL) measurement was carried out with a JY-630 micro-Raman spectrometer employing the 325 nm line of a He–Cd laser as the excitation source, and the room temperature Raman spectra were recorded using the same micro-Raman spectrometer with a 488 nm excitation source. The current–voltage characteristics of the crossed p–n homojunction device were measured using a Keithley 2611A measurement system. The photoresponse of the crossed p–n homojunction device was measured with a 150 W Xe lamp, chopper (EG&G192), and lock-in amplifier (EG&G1 24A) at room temperature.

3. Results and discussion

3.1 Structural and optical properties

Fig. 1 shows the FE-SEM images of both undoped and Sb-doped ultralong ZnO microwires. The microwires are up to 10 millimeters in length. Fig. 1a is the SEM image of an undoped ZnO microwire with a square cross-section. In Fig. 1b, the Sb-doped ZnO microwire keeps the same square cross-section structure. But the surface morphology changes distinctly due to the incorporation of the Sb dopant, which presents a zigzag rough surface compared to the smooth surface of the undoped ZnO microwire. The details of the zigzag rough surface could be obviously seen in the enlarged SEM image shown in the inset of Fig. 1b (bottom). Since the radius of Sb^{3+} (0.78 Å) is much larger than that of Zn^{2+} (0.74 Å), the introduction of Sb atoms would cause a large structural strain, the release of the structural strain could result in the formation of the planar defects.[18] In addition, the synthesis temperature of the substrate is as high as 1000 °C, which is much higher than the melt point of Sb_2O_3, therefore the origination of the zigzag rough surface in ZnO microwires could be attributed to the introduction of Sb dopants. The doping of the Sb element is responsible for the formation of the zigzag surface in ZnO microwires, which is in accordance with the literature.[18,36] To determine the composition of Sb in ZnO microwires, we performed the EDX analysis, which showed that the Sb concentration was 0.3% within the measurement limit of EDX. The zigzag rough surface is even along the whole microwire, which implies the uniform Sb doping in ZnO. The SAED pattern of the Sb-doped ZnO microwire is shown in the inset of Fig. 1b (top), which confirms that the Sb-doped ZnO microwire is single crystalline.

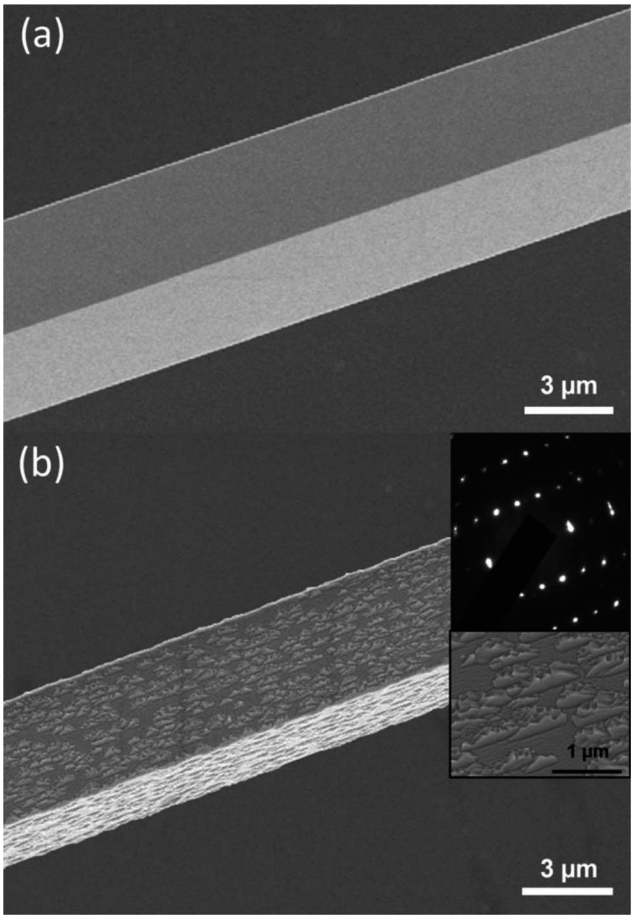

Fig. 1 (a) SEM image of the undoped ZnO microwire shows a smooth surface. (b) SEM image of the Sb-doped ZnO microwire shows a zigzag rough surface. Inset: top: SAED pattern of the Sb-doped ZnO microwire showed a single crystalline structure; bottom: the enlarged SEM image of Sb-doped ZnO microwires.

Fig. 2a shows the low-temperature (at 85 K) PL spectra of undoped and Sb-doped ZnO microwires. The emission peak of the undoped ZnO microwire located at 3.360 eV is assigned to the recombination of the shallow donor-bound exciton (D_0X).[19] The small peak at 3.378 eV originates from the recombination of the free exciton A (FX_A). The peak located at 3.318 eV is

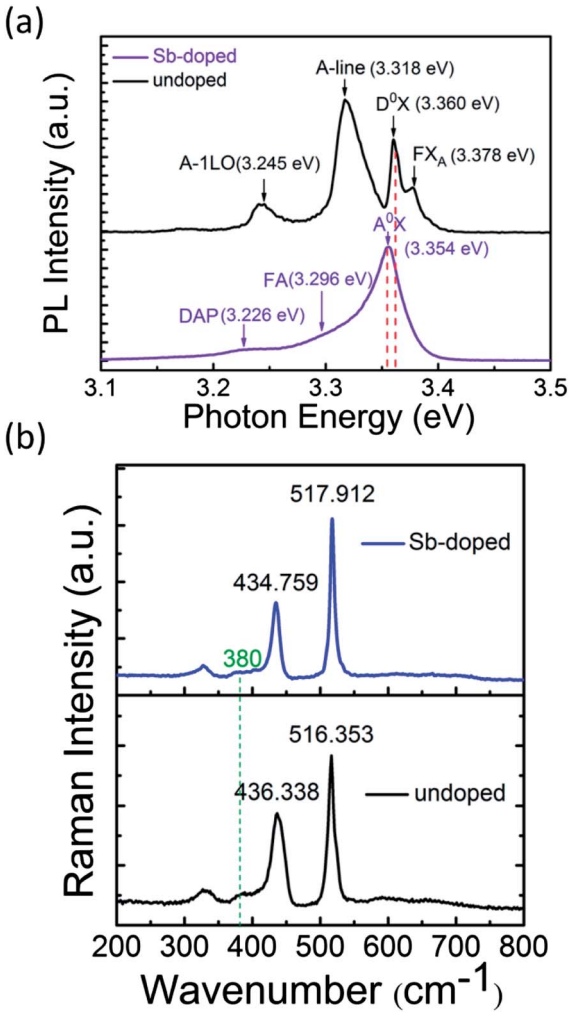

Fig. 2 (a) Low temperature PL spectra of undoped (top curve) and Sb-doped (bottom curve) ZnO microwires at 85 K. The doped microwire showed acceptor related emissions. (b) Raman spectra of Sb-doped and undoped ZnO microwires indicate that the Sb dopant has been incorporated into ZnO and introduced acceptor levels.

attributed to A-line emission. The origin of the A-line emission is currently under discussion; it has some possible assignments including neutral excitons bound to nitrogen impurities, excitons bound to surface or structural defects, and two-electron transition of the exciton bound to the neutral donor.[20] The small peak at 3.245 eV is the 1-LO phonon replicas of the A-line emission, since it is 73 meV lower than the A-line peak. For Sb-doped ZnO microwires, the low-temperature PL spectrum shows a dominated emission peak centered at 3.354 eV, which is associated with the neutral-acceptor-bound exciton (A_0X) recombination.[21,22] The emission peaks located at 3.296 eV and 3.226 eV are ascribed to the free electron to acceptor (FA) and donor–acceptor–pair (DAP) transitions, respectively.[23] Room temperature Raman spectra were measured to further confirm the incorporation of Sb atoms into the ZnO microwire lattices, since it is an effective analysis method to study the impurity induced modes. As shown in Fig. 2b, the peak at 380 cm^{-1} which corresponds to the A_{1T} modes in ZnO is depressed by Sb doping. Since the oxygen defect or the dopant atom directly affects the A_{1T} modes, Sb dopant atoms would be responsible for the depression in 380 cm^{-1}.[24] The peak centered at 436 cm^{-1} is usually attributed to the E_2 modes of the undoped ZnO single crystal, and this peak shifts toward lower frequency to 434 cm^{-1} when doping with Sb, which is caused by the formation of the Sb_{Zn}–$2V_{Zn}$ complex acceptor in Sb-doped ZnO microwires.[25] Sb_{Zn}–$2V_{Zn}$ was demonstrated to have both low formation energy and low ionization in ZnO lattices and represented the shallow acceptor defect levels.[26] Consequently, low-temperature PL and Raman spectra studies reveal that Sb was incorporated into ZnO crystal lattices which generated acceptor-associated defect levels in Sb-doped ZnO microwires.

3.2 Electrical properties

The electrical measurements on ZnO microwire back-gated field-effect transistors (FETs) were carried out to confirm the conductivity type of the as-synthesized Sb-doped ZnO microwires. FETs in our study were fabricated using both undoped and Sb-doped ZnO microwires; the microwires were transferred on the p^+-silicon wafer covered with a 300 nm thick SiO_2 film. The p^+-silicon substrate and the SiO_2 layer served as the back-gate electrode and dielectric gate oxide of FETs, respectively. Indium (In) electrodes were deposited on the two ends of the microwires to form Ohmic contacts. Fig. 3a and b show the output characteristics at various back-gate voltages of a single Sb-doped and undoped ZnO microwire, respectively. In Fig. 3a, the increase of the drain–source current (I_{ds}) with an increasingly negative gate voltage clearly indicates the p-type conduction of the Sb-doped ZnO microwire.[27,28] By comparison, the increase of I_{ds} with an increasingly positive gate voltage of undoped ZnO presents n-type conductivity.

A ZnO microwire p–n homojunction was designed and fabricated as shown in the schematic diagram in Fig. 4a. Current–voltage (I–V) characteristics of the constructed homojunction are depicted in Fig. 4b. Well-defined current rectification characteristics are observed in this cross-structured microwire p–n homojunction device, the turn-on voltage is around 5 V. As shown in the inset of Fig. 4b, transport data recorded on the individual p-type and n-type ZnO microwires both exhibit linear behaviour, therefore good Ohmic contacts are established on both n-type and p-type ZnO microwires with In electrodes. To prove that the rectification behaviour of the p–n junction does not result from the influence of the interface between two microwires; I–V characteristics of the n–n junction configured by crossing two n-type ZnO microwires were also investigated. In the inset of Fig. 4b, transport measurement carried out on the n–n junction shows nearly linear behaviour, which indicates that the interface between individual n-type microwires does not produce a nonlinear curve. Moreover, the currents recorded through the p–n junction and n–n junction are much smaller than through individual p-type and n-type ZnO microwires at the same voltage, which demonstrates that the junction dominates the transport behaviour.[29] Consequently, the rectification can be definitely attributed to the crossed p–n homojunction.

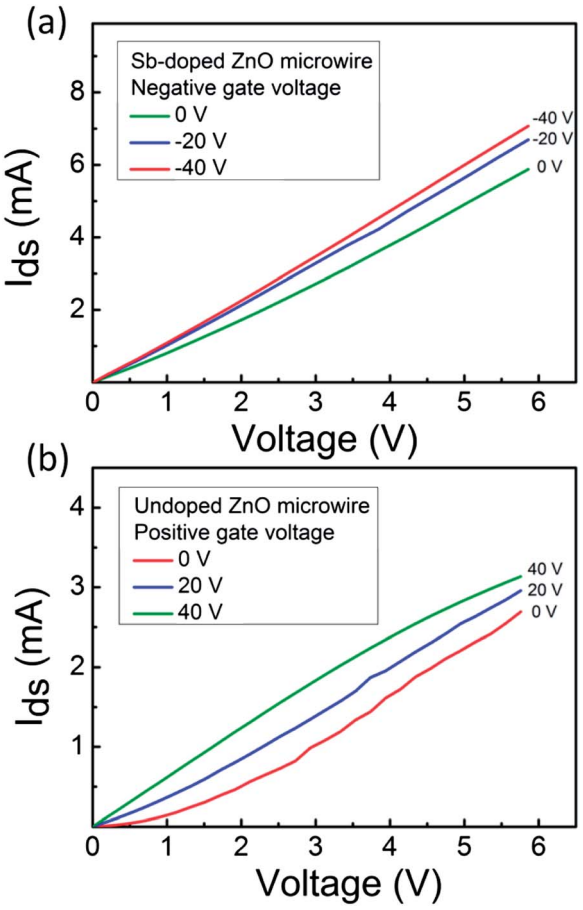

Fig. 3 Output characteristics at various back-gate voltages of ZnO microwire FETs. (a) I_{ds} *versus* V_{ds} curves at various negative gate voltages of a single Sb-doped ZnO microwire FET showed p-type conductivity. (b) I_{ds} *versus* V_{ds} curves at various positive gate voltages of an undoped ZnO microwire FET showed n-type conductivity.

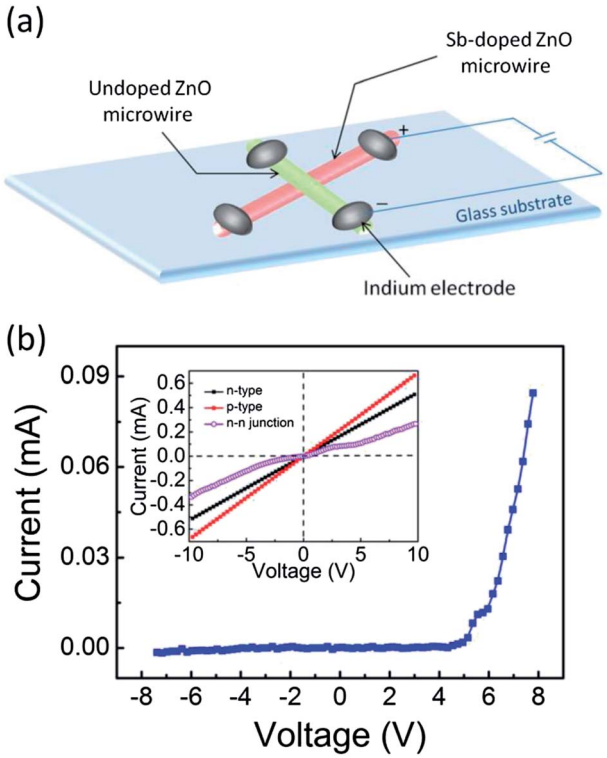

Fig. 4 (a) Structure illustration of the crossed ZnO microwire p–n homojunction device. (b) *I–V* characteristics of the crossed ZnO microwire p–n homojunction. Inset: *I–V* characteristics of individual n-type (black), p-type (red) ZnO microwires, and crossed two single n-type ZnO microwires' n–n junction (purple).

3.3 ZnO microwire homojunction UV photodetector

The ZnO microwire p–n homojunction could be utilized as a highly efficient UV photodetector. *I–V* characteristics of the ZnO microwire p–n homojunction in the dark and under UV illumination are shown in Fig. 5a; the photocurrent increases remarkably under the reverse voltage by 365 nm UV illumination (1.21 mW cm^{-2}). The current gain of a p–n junction detector (not an avalanche photodiode[30,31]) is usually equal to 1, thus the photocurrent could be expressed as:

$$I_{ph} = \eta q \Phi \quad (1)$$

where η is the EQE, q is the electron charge, and Φ is the photon flux density.[32] As displayed in eqn (1), the photocurrent is strongly related to the EQE of the detector.

Fig. 5b shows the photoresponse spectrum of the ZnO microwire p–n homojunction at −4 V bias. The photoresponse peak is located at 386 nm, which is 2 orders of magnitude higher than the responsivity of visible light. The FWHM of the photoresponse peak of about 6 nm shows the high wavelength selectivity which profits from the high crystalline quality of the ZnO microwire. ZnO material is transparent in visible light; the electron–hole pairs with energy less than the bandgap cannot be excited by the incident light and thus contribute little to photocurrent. Meanwhile, the device shows nearly no response on the shorter wavelength side smaller than 380 nm, which is attributed to the enhanced absorption of high-energy photons with energy higher than the bandgap at or near the surface of the semiconductor. Electron–hole pairs generated near the surface region have a shorter lifetime,[35] which decreases the efficient electron–hole separation for incident photons. Therefore the electron–hole pairs with large energies will not contribute to the photoresponse. Consequently, the ZnO microwire p–n homojunction photodetector shows a high wavelength selectivity.

The inset of Fig. 5b shows the responsivity of the ZnO microwire p–n homojunction UV photodetector as a function of applied bias; the responsivity goes up gradually as the applied reverse bias; the peak responsivity is 200 mA W^{-1} at 386 nm under −5 V bias. The current responsivity of the p–n junction detector is defined as:

$$R(A/W) = \frac{I_{ph}}{P_{opt}} = \eta\left(\frac{q\lambda}{hc}\right) \quad (2)$$

where I_{ph} is the photocurrent, P_{opt} is the incident optical power, η is the EQE, h is Planck's constant, c is the speed of light, λ is the incident light wavelength, and q is the electron charge.[32] According to eqn (2), the EQE was calculated to be 64.5%, which indicates that the ZnO microwire p–n homojunction photodetector has excellent UV photoresponse characters.

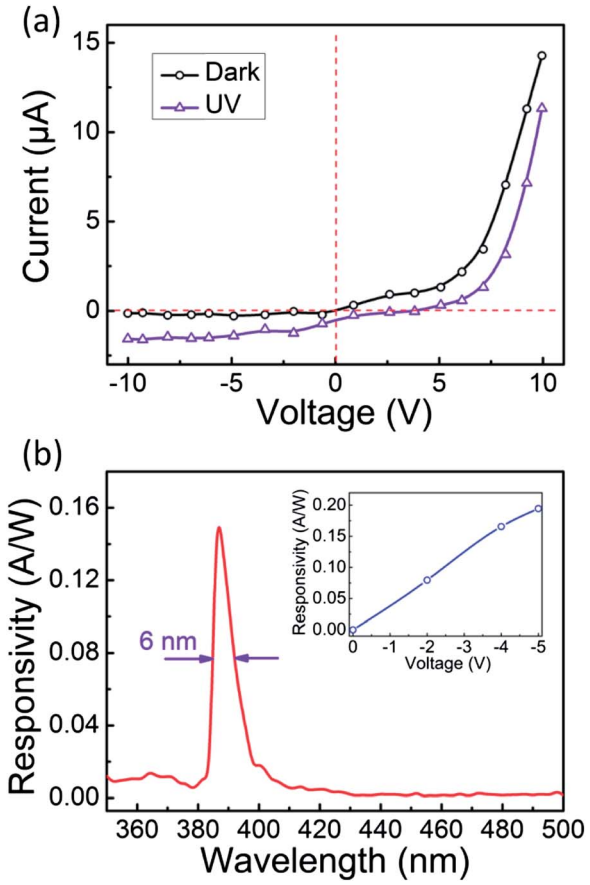

Fig. 5 (a) *I–V* characteristics of the crossed ZnO microwire p–n homojunction with and without UV illumination. (b) Response spectrum of the crossed-wire photodetector under −4V bias. Inset: the maximum responsivity of the device as a function of the applied reverse bias.

4. Conclusions

A ZnO microwire p–n homojunction UV photodetector with high efficiency and high wavelength selectivity has been demonstrated. The photodetector was formed by a single Sb-doped ZnO microwire and a single undoped ZnO microwire. Sb-doped p-type ZnO microwires were synthesized by a CVD method; the morphology changed distinctly due to Sb incorporation. Low-temperature PL and Raman spectra measurements showed that a shallow acceptor was formed in the Sb-doped ZnO microwire. A fine rectification character was obtained on the ZnO microwire p–n homojunction indicating the p-type conductivity of the Sb-doped ZnO microwire. The UV photodetector exhibited high wavelength selectivity and the FWHM was only 6 nm. The peak responsivity of 200 mW^{-1} was measured at a wavelength of 386 nm under −5 V voltage, which corresponds to a high EQE of 64.5%.

Acknowledgements

This work was supported by the National Basic Research Program of China (973 Program) under Grant nos 2011CB302006, 2011CB302005, and 2011CB302004, the National Science Foundation of China under Grant nos 11074248, 10974197, 11104265, and 61376054, and the 100 Talents Program of the Chinese Academy of Sciences.

Notes and references

1 A. Tsukazaki, A. Ohtomo, T. Onuma, M. Ohtani, T. Makino, M. Sumiya, K. Ohtani, S. F. Chichibu, S. Fuke, Y. Segawa, H. Ohno, H. Koinuma and M. Kawasak, *Nat. Mater.*, 2005, **4**, 42.
2 X. M. Zhang, M. Y. Lu, Y. Zhang, L. J. Chen and Z. L. Wang, *Adv. Mater.*, 2009, **21**, 2767.
3 M. H. Huang, S. Mao, H. Feick, H. Yan, Y. Wu, H. Kind, E. Weber, R. Russo and P. D. Yang, *Science*, 2001, **292**, 1897.
4 O. Lupan, T. Pauporté and B. Viana, *Adv. Mater.*, 2010, **22**, 3298.
5 H. Kind, H. Q. Yan, B. Messer, M. Law and P. D. Yang, *Adv. Mater.*, 2002, **14**, 158.
6 S. Liang, H. Sheng, Y. Liu, Z. Huo, Y. Lu and H. Shen, *J. Cryst. Growth*, 2001, **225**, 110.
7 C. Soci, A. Zhang, B. Xiang, S. A. Dayeh, D. P. R. Aplin, J. Park, X. Y. Bao, Y. H. Lo and D. Wang, *Nano Lett.*, 2007, **7**, 1003.
8 D. C. Look, *Mater. Sci. Eng., B.*, 2001, **80**, 383.
9 Y. Z. Jin, J. P. Wang, B. Q. Sun, J. C. Blakesley and N. C. Greenham, *Nano Lett.*, 2008, **8**, 1649.
10 J. H. He, Y. H. Lin, M. E. McConney, V. V. Tsukruk, Z. L. Wang and G. Bao, *J. Appl. Phys.*, 2007, **102**, 084303.
11 J. Zhou, Y. D. Gu, Y. F. Hu, W. J. Mai, P. H. Yeh, G. Bao, A. K. Sood, D. L. Polla and Z. L. Wang, *Appl. Phys. Lett.*, 2009, **94**, 191103.
12 Y. F. Hu, J. Zhou, P. H. Yeh, Z. Li, T. Y. Wei and Z. L. Wang, *Adv. Mater.*, 2010, **22**, 3327.
13 C. S. Lao, J. Liu, P. X. Gao, L. Y. Zhang, D. Davidovic, R. Tummala and Z. L. Wang, *Nano Lett.*, 2006, **6**, 263.
14 K. C. Pradel, W. Z. Wu, Y. S. Zhou, X. N. Wen, Y. Ding and Z. L. Wang, *Nano Lett.*, 2013, **13**, 2647.
15 W. J. Chen, J. K. Wu, J. C. Lin, S. T. Lo, H. D. Lin, D. R. Hang, M. F. Shih, C. T. Liang and Y. H. Chang, *Nanoscale Res. Lett.*, 2013, **8**, 313.
16 G. P. Wang, S. Chu, N. Zhan, Y. Q. Lin, L. Chernyak and J. L. Liu, *Appl. Phys. Lett.*, 2011, **98**, 041107.
17 S. Chu, G. P. Wang, W. H. Zhou, Y. Q. Lin, L. Chernyak, J. Z. Zhao, J. Y. Kong, L. Li, J. J. Ren and J. L. Liu, *Nat. Nanotechnol.*, 2011, **97**, 1.
18 Y. Yang, J. J. Qi, Q. L. Liao, Y. Zhang, L. D. Tang and Z. Qin, *J. Phys. Chem. C*, 2008, **112**, 17916.
19 A. Teke, Ü. Özgür, S. Do ğan, X. Gu and H. Morkoç, *Phys. Rev. B: Condens. Matter Mater. Phys.*, 2004, **70**, 195207.
20 S. S. Kurbanov, G. N. Panin and T. W. Kang, *Appl. Phys. Lett.*, 2009, **95**, 211902.
21 E. Przeździecka, E. Kamińska, I. Pasternak, A. Piotrowska and J. Kossu, *Phys. Rev. B: Condens. Matter Mater. Phys.*, 2007, **76**, 193303.
22 K. Samanta, A. K. Arora, S. Hussain, S. Chakravarty and R. S. Katiyar, *Curr. Appl. Phys.*, 2012, **12**, 1381.

23 F. X. Xiu, Z. Yang, L. J. Mandalapu, D. T. Zhao and J. L. Liu, *Appl. Phys. Lett.*, 2005, **87**, 252102.
24 I. A. Palani, K. Okazaki, D. Nakamura, K. Sakai, M. Higashihata and T. Okada, *Appl. Surf. Sci.*, 2012, **258**, 361.
25 K. Samanta, P. Bhattacharya and R. S. Katiyar, *J. Appl. Phys.*, 2010, **108**, 113501.
26 S. Limpijumnong, S. B. Zhang, S. H. Wei and C. H. Park, *Phys. Rev. Lett.*, 2004, **92**, 155504.
27 W. Liu, F. X. Xiu, K. Sun, Y. H. Xie, K. L. Wang, Y. Wang, J. Zou, Z. Yang and J. L. Liu, *J. Am. Chem. Soc.*, 2010, **132**, 2498.
28 A. B. Yankovich, B. Puchala, F. Wang, J. H. Seo, D. Morgan, X. D. Wang, Z. Q. Ma, A. V. Kvit and P. M. Voyles, *Nano Lett.*, 2012, **12**, 1311.
29 X. F. Duan, Y. Huang, Y. Cui, J. F. Wang and C. M. Lieber, *Nature*, 2001, **409**, 66.
30 O. Hayden, R. Agarwal and C. M. Lieber, *Nat. Mater.*, 2006, **5**, 352.
31 C. Yang, C. J. Barrelet, F. Capasso and C. M. Lieber, *Nano Lett.*, 2006, **6**, 2929.
32 S. M. Sze, *Physics of Semiconductor Devices*, John Wiley and Sons, Inc., New York, 1981.
33 Y. Q. Bie, Z. M. Liao, H. Z. Zhang, G. R. Li, Y. Ye, Y. B. Zhou, J. Xu, Z. X. Qin, L. Dai and D. P. Yu, *Adv. Mater.*, 2011, **23**, 649.
34 Q. Chen, H. Y. Ding, Y. K. Wu, M. Sui, W. Lu, B. Wang, W. M. Su, Z. Cui and L. W. Chen, *Nanoscale*, 2013, **5**, 4162.
35 J. S. Jie, W. J. Zhang, Y. Jiang, X. M. Meng, Y. Q. Li and S. T. Lee, *Nano Lett.*, 2006, **6**, 1887.
36 B. C. Cheng, B. X. Tian, W. Sun, Y. H. Xiao, S. J. Lei and Z. G. Wang, *J. Phys. Chem. C*, 2009, **113**, 9638.